Biophysical Chemistry 172 (2013) 37–42

Contents lists available at SciVerse ScienceDirect

Biophysical Chemistry

journal homepage: http://www.elsevier.com/locate/biophyschem

How does overcoordination create ion selectivity?

Michael Thomas [a], Dylan Jayatilaka [b], Ben Corry [a,*]

[a] Research School of Biology, The Australian National University, Canberra, Australia
[b] School of Chemistry and Biochemistry, University of Western Australia, Perth, Australia

HIGHLIGHTS

- We describe how ion selectivity can arise by 'overcoordination'.
- There is a point at which the ligands form a 'full' shell around an ion.
- This happens with a lower number of ligands for smaller ions.
- Beyond this, adding ligands significantly changes the positions of all the ligands.
- Selectivity arises when this point has been reached for one ion but not another.

GRAPHICAL ABSTRACT

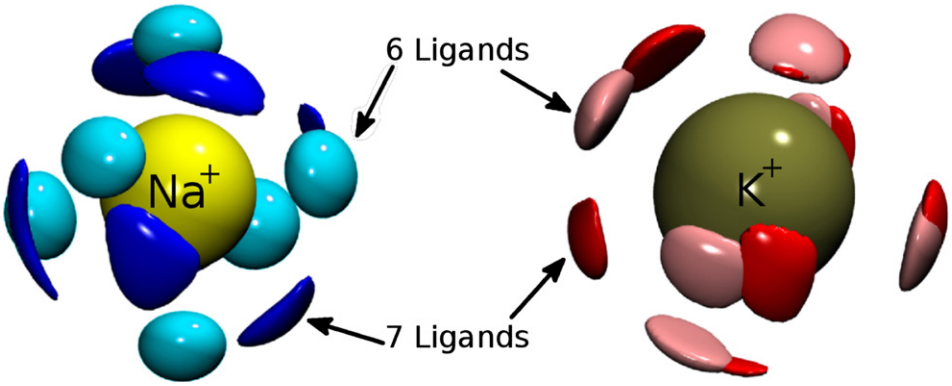

ARTICLE INFO

Article history:
Received 12 October 2012
Received in revised form 20 November 2012
Accepted 23 November 2012
Available online 4 December 2012

Keywords:
Ion selectivity
Overcoordination
Molecular dynamics simulation

ABSTRACT

Some biological molecules can distinguish between ions of similar nature, which may be achieved by enforcing specific coordination numbers on ions in the binding site. It is suggested that when this number is favourable for one ion type, but too large for another, this creates ion selectivity through the proposed mechanism of 'overcoordination'. Much debate has occurred about the role overcoordination plays, and suggestions made as to how molecules can enforce particular coordination numbers, but there has not been an examination of the microscopic underpinning of ion selectivity by overcoordination. Here we use molecular-dynamics to systematically investigate how the number of ligands affects the ion–ligand and ligand–ligand interaction energies, and thus the thermodynamic ion selectivity, of a combination of model systems: three ions ($Li^+/Na^+/K^+$) with three different ligands (water/formaldehyde/formamide). We find that the ligand–ligand repulsion controls the changes in geometry of each system with changing ligand number. Ion selectivity by overcoordination is achieved as smaller ions exhibit anomalous geometrical changes with the addition of extra ligands, whilst larger ions do not.

1. Introduction

The ability of proteins to discriminate between ions is integral to many biological processes, such as enzyme function and the regulation of membrane potentials [1]. One well studied example of ion differentiation arises in the exquisitely selective potassium ion channels.

* Corresponding author at: Research School of Biology, The Australian National University, Canberra, ACT 0200, Australia. Tel.: +61 2 6125 0842.
E-mail address: ben.corry@anu.edu.au (B. Corry).

0301-4622/$ – see front matter © 2012 Elsevier B.V. All rights reserved.
http://dx.doi.org/10.1016/j.bpc.2012.11.005

These channels display up to a 1000 fold preference for K^+ over Na^+ [2–5], despite the fact that the two ions are both spherical in nature, have the same charge and differ in atomic radii by only 0.38 Å. Whilst a range of mechanisms have been put forward to explain selectivity in potassium channels, including the snug-fit hypothesis [6–10], the chemical nature of the coordinating ligands [11–17] and the more recent kinetic hypothesis based on different binding sites for Na^+ and K^+ [18–20], a number of studies suggest that 'overcoordination' plays a role in ion discrimination in the potassium channel KcsA [16,17,21–31]. Overcoordination arises when the chemical environment enforces a large coordination number on ions in a binding site that is thermodynamically less favourable for one ion than another.

A number of studies have addressed two key questions about ion selectivity by overcoordination:

1. How important is overcoordination in establishing ion selectivity in a particular molecule [17,21,22,25,28–30]? This question has been extensively investigated in regard to selectivity in K^+ channels; if selectivity is achieved via a thermodynamic mechanism (and not a kinetic mechanism as suggested by some recent studies [18–20]), the literature seems to point to overcoordination playing an important role.
2. By what means are these molecules able to enforce a particular coordination number? Here the focus is on mechanisms that can constrain the position of the coordinating ligands. An example of this is the hydrogen bonding networks present in K^+ channels that could act as a radial spring on the coordinating ligands, thus enforcing a large coordination number [10]. Also, it has been suggested that the lack of hydrogen bond donors keeps the carbonyl oxygens that line the selectivity filter in K^+ channels free to coordinate the permeating ions [27].

In contrast to these questions that have been much studied in the literature, a third key issue relating to ion selectivity by overcoordination has received surprisingly little attention:

3. Through what physical means does enforcing a coordination number create ion selectivity? Whilst it is known that a large number of coordinating ligands produce more favourable interactions for larger ions than smaller, what physical phenomena give rise to this? Perhaps the explanation is obvious, but to the best of our knowledge this issue has not been addressed head on and systematically studied.

In this study, we do not attempt to answer the first and second questions, but instead focus on the third question: determining the microscopic basis of the concept of ion selectivity by overcoordination.

Studies conducted by Noskov et al. [13,14] investigated the interplay of ion–ligand and ligand–ligand interactions in search of the cause of selectivity in potassium ion channels. It was concluded that the geometry of the ion binding site is governed by the ion–ligand interaction, whilst the ligand–ligand interaction influences ion selectivity [13] and that these "can be directly modulated by the number and the type of ligands involved in ion coordination" [14]. However, what we wish to study is how these interactions and ion selectivity vary with the number of ligands coordinating to an ion, not how a particular binding site achieves selectivity.

The aim of this study is not to reproduce the properties of any particular binding site, but to use simplistic systems to investigate in principle how coordination numbers can influence ion selectivity. As coordination does influence selectivity in these models, we can examine why this is the case. Some of these factors may play a role in biological systems. We employ three simple ligands to examine the effect of the chemical nature of the binding site, but do not explicitly include structural or environmental factors that are likely to be at play in a real ion binding molecule.

The methods employed in this study are classical molecular dynamics techniques utilising a non-polarisable force field [32], which has been shown to produce ion partitioning between bulk liquids, such as formaldehyde and water [17], and *N*-methylacetamide and water [13]. Ion selectivity by overcoordination is readily apparent from the simulations conducted here, in addition to similar simulations in previous work [17,21]. More detailed investigations (such as those employing polarisable force fields or quantum mechanical calculations) may illuminate additional effects not captured here. However, given that ion selectivity is apparent in our classical model, we can understand the mechanisms that lead to selectivity in this situation.

To investigate why overcoordination creates selectivity, free energy perturbation (FEP) MD simulations were conducted on a series of model systems. These consisted of either n water, formaldehyde or formamide molecules whose oxygen atoms were constrained to a 3.5 Å sphere about either Li^+, Na^+, and K^+ (for $n = 1$–10). This distance represents the first minimum in the radial distribution function of K^+ in bulk water. The constraining sphere acts to hold a number of ligands near the ion whilst allowing the ligands to adjust their relative positions. Inside this sphere, the ligands are completely free to move about, very different from the snug-fit mechanism where ligands are constrained to particular positions. Strictly enforcing the coordination number would require a different radius of constraint for each ion type, to keep each ligand in the inner shell. However, we feel that the use of a single radius best represents binding sites in molecules, as the molecular scaffold that holds the ligands near the ion is the same

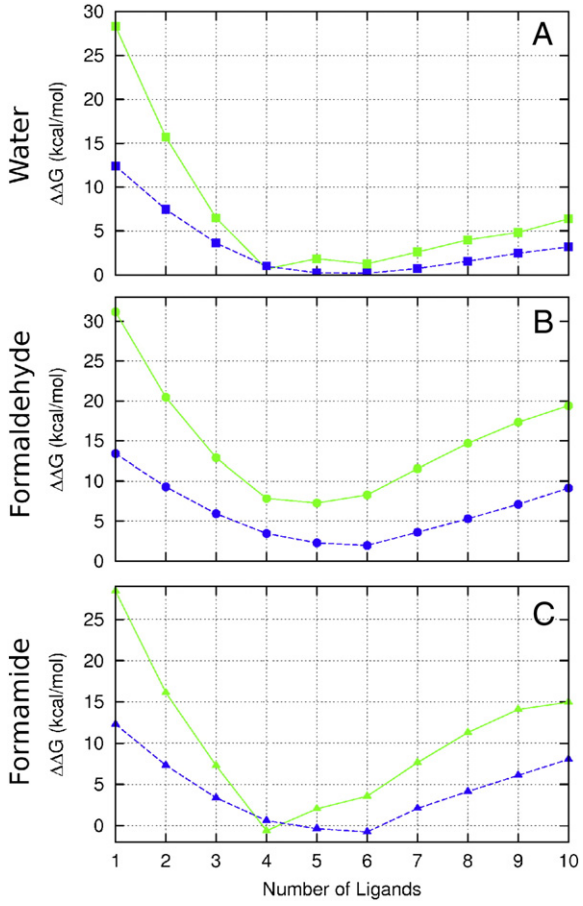

Fig. 1. Relative free energy values, $\Delta\Delta G(Na^+,K^+) = \Delta G_{site}(Na^+ \rightarrow K^+) - \Delta G_{Bulk}(Na^+ \rightarrow K^+)$ of the exchange reaction between Li^+ and K^+ (green), Na^+ and K^+ (blue) and K^+ and itself (which by definition is zero), in model binding sites with varying number of ligands, n, and bulk water. The three types of ligands that are modelled are (A) water, (B) formaldehyde and (C) formamide. A positive value indicates that K^+ is preferred over the other ion in the model site.

regardless of ion type. The free energy change for ion exchange with bulk water for each system was determined. As the entropic contributions to ion selectivity are known to be small in these types of systems [14,15,33,34], a decomposition of the energy into average ion–ligand and ligand–ligand contribution (as interaction energies) will provide insight into the forces at play. Average ion–ligand and ligand–ligand distances were also measured from the simulations.

2. Results and discussion

It has been previously demonstrated that constraining the coordination number of ions in a binding site can create ion selectivity [13,14,17,21,22,27,29,30], as is shown in Fig. 1. Here the ion selectivity obtained with each ligand type (formaldehyde, water and formamide) is shown relative to K^+ for each of the model binding sites, assuming that each ion has to leave bulk water to enter the site. In all cases, enforcing a large coordination number favours K^+, the larger ion. The binding sites that are the least selective for K^+ over Li^+ are 4-fold coordination for water and formamide ligands, and 5-fold coordination for formaldehyde ligands. For all ligand types, the binding site is least selective for K^+ over Na^+ when 6 ligands are present. Fig. 1 also shows that small coordination numbers (undercoordination) also favour large ions, but for a different reason: the inability to recoup the larger dehydration energy of the smaller ion.

Electrostatically each ion in this study is identical in our classical force field, thus the only difference between Na^+ and K^+ in the model is the Lennard–Jones potential, which reflects ion size. The repulsion term prohibits the K^+–oxygen distance from becoming as small as the Na^+–oxygen or Li^+–oxygen distance. Conversely, it allows Li^+ to adopt smaller ion–ligand distances for small numbers of ligands. We next aim to determine how the difference in ion–ligand geometries affects energetics and selectivity.

To understand how enforcing a particular coordination number creates ion selectivity, we follow Noskov and Roux [14] in decomposing the total energy into ion–ligand and ligand–ligand interactions as shown in Fig. 2, plotted as the coordination number n is increased from 1 to 10. As one would expect, the ion–ligand interaction is attractive, which generally increases in strength as n increases. The ligand–ligand interaction is repulsive for formaldehyde and water, whilst being attractive for formamide, due to the ease of establishing hydrogen bonding between ligands in this case. However, the ligands' ability to hydrogen bond may be diminished if they linked as in a polypeptide chain. Even though this term is attractive for formaldehyde, there is still a strong repulsion between the oxygen atoms coordinating to the ion. The ligand–ligand interaction energies change monotonically for formaldehyde and formamide, whereas water increases, then decreases, forming a peak about $n=6$. The reason for this behaviour in water is that it is more energetically favourable for the water ligands to begin forming a second solvation shell within the 3.5 Å constraint for $n\geq 6$ than it is to add an additional ligand into the first solvation shell (see Fig. S1).

A more informative analysis of the interaction results if we plot the change in each energy component when an additional ligand is added to the site (effectively a derivative of Fig. 2). Fig. 3 shows this difference in energy, $\Delta E = E_n - E_{n-1}$, from which two features are apparent. Firstly, the change in ligand-ligand interaction arising from adding an additional ligand peaks when the systems reach the 5th or 6th ligand (depending on the system in question). Secondly, and more important, is the sharp increase in the ΔE for the ion–ligand interaction seen for Li^+ and to a smaller extent Na^+ compared to that of K^+ at specific ligand numbers. For example, in Fig. 3D, the addition of the 5th and 7th formaldehyde ligands for Li^+ and the 7th ligand for Na^+ dramatically decreases the rate at which this interaction stabilises the coordination system. This anomalous change in the ion–ligand interaction leads to a similar change in the total energy (Fig. 3F for example) found when adding an extra ligand to the system. Analogous situations arise for water and formamide. The major contribution to changes to the relative energies of the ion/ligand

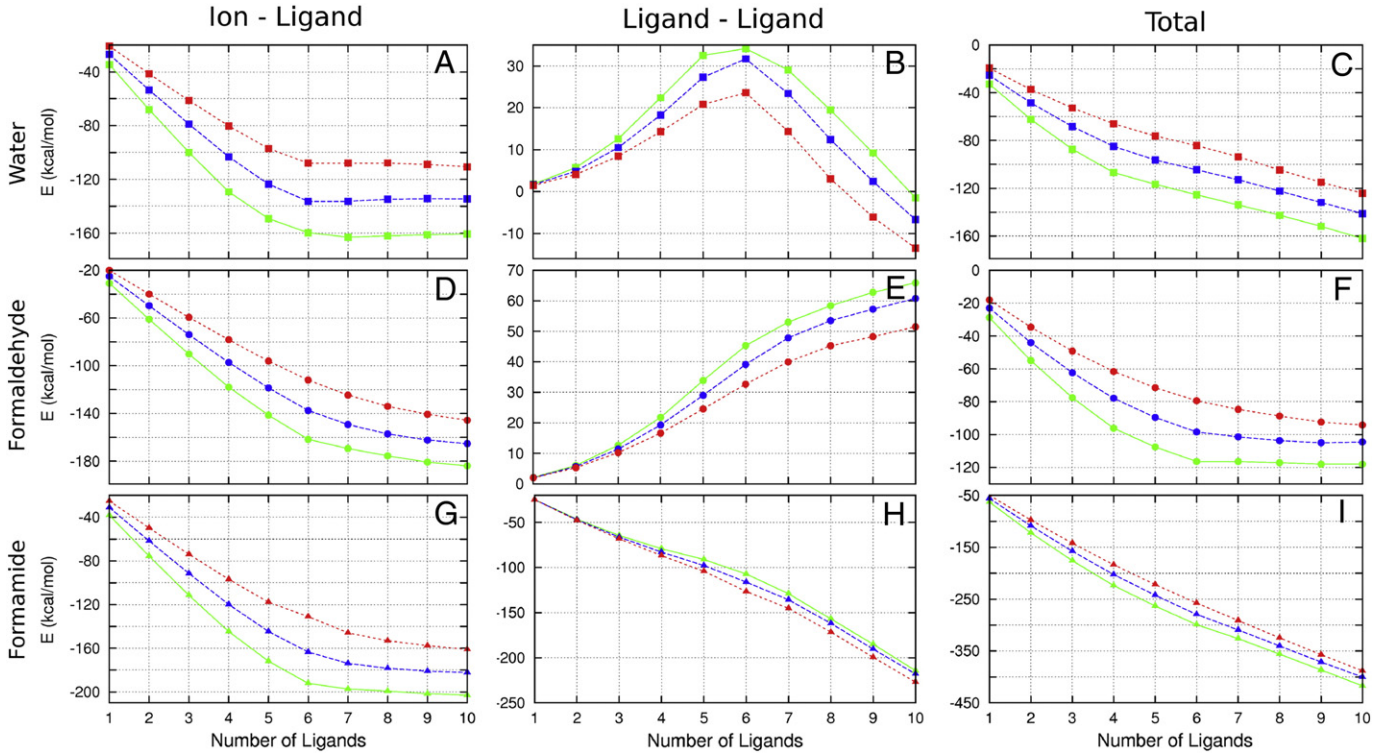

Fig. 2. Average ion–ligand, ligand–ligand and total interaction energies are shown for ions (Li^+ (green), Na^+ (blue) and K^+ (red)) in water (A, B, C), formaldehyde (D, E, F) and formamide (G, H, I).

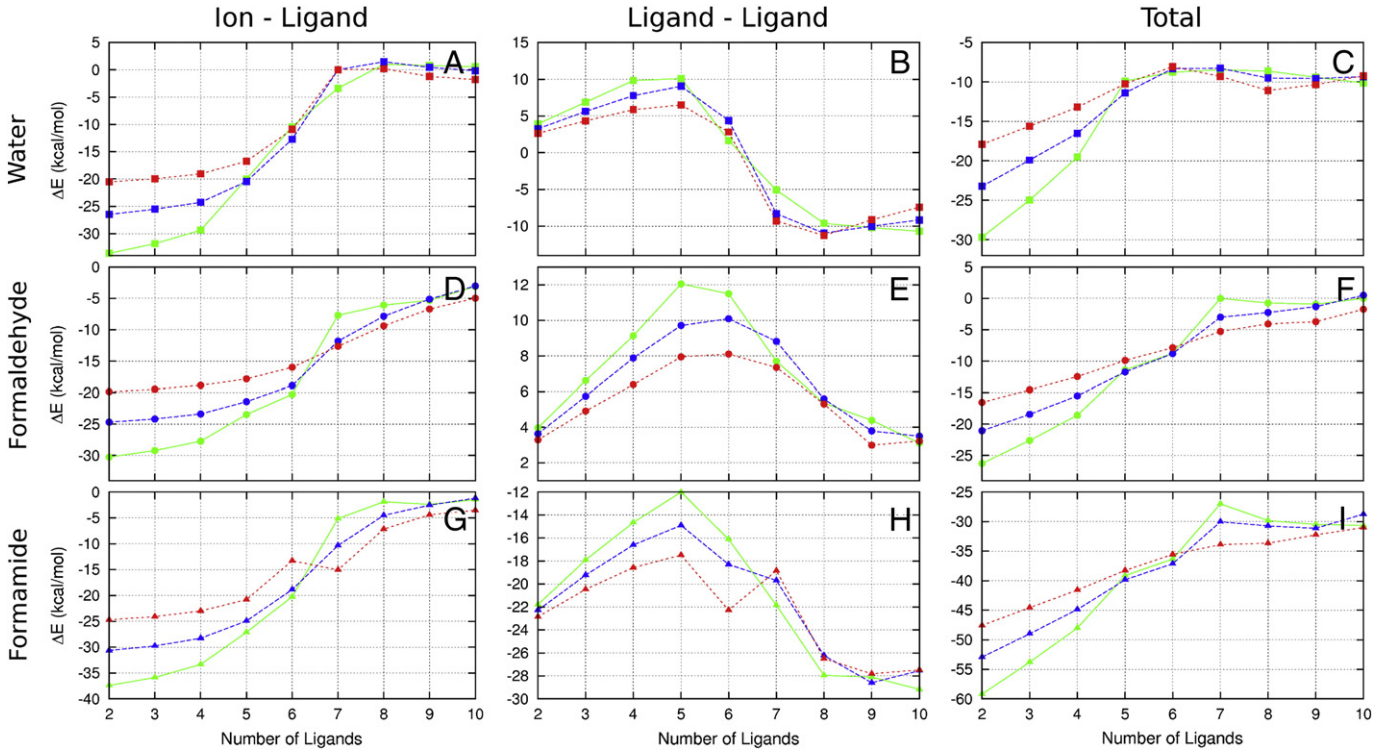

Fig. 3. Change in average energies, $\Delta E = E_n - E_{n-1}$, for ion–ligand, ligand–ligand and total interactions are shown for ions (Li^+ (green), Na^+ (blue) and K^+ (red)) in water (A, B, C), formaldehyde (D, E, F) and formamide (G, H, I).

systems when n changes from 4 to 8 originates from these sharp changes in the ion–ligand interaction energy at $n = 5$ and $n = 7$.

What is happening at these specific coordination numbers to cause the ion–ligand interaction energy to change in this way? Fig. 4A, C and E plots the change in the average ion–oxygen distance with an increase in coordination number, Δr, against the coordination number for each ion and each ligand type. Marked differences between the results for the three ions can be seen. For each ligand

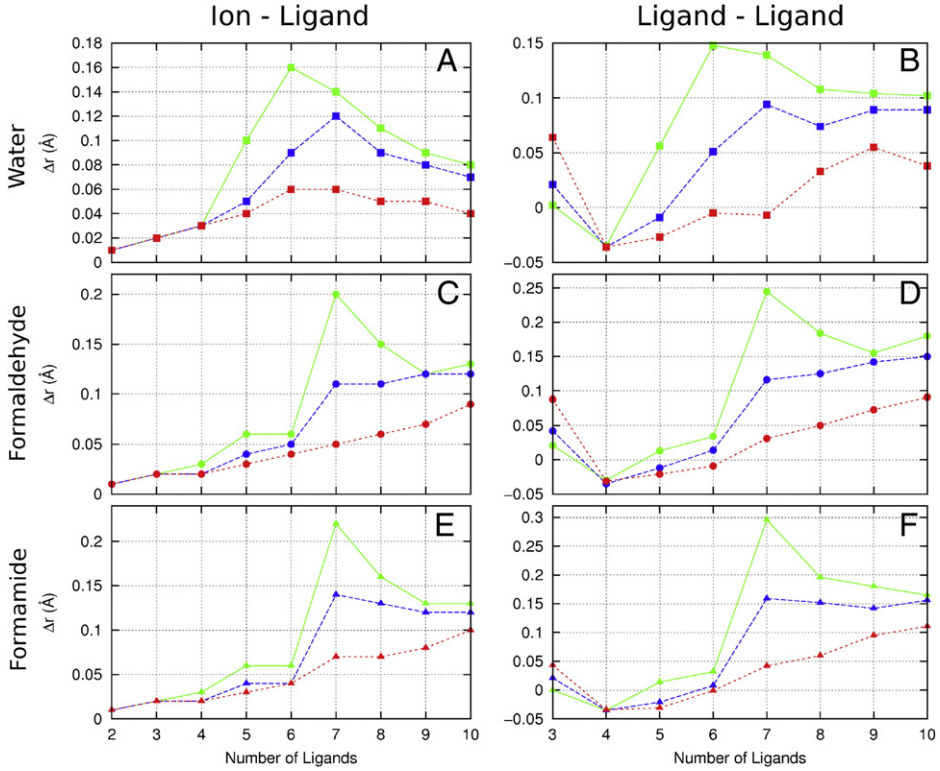

Fig. 4. Changes in average ion–ligand distance, $\Delta r = r_n - r_{n-1}$ for Li^+ (green), Na^+ (blue) and K^+ (red) with (A) water, (C) formaldehyde and (E) formamide. Changes in the average ligand–ligand distance for Li^+, Na^+ and K^+ with (B) water, (D) formaldehyde and (F) formamide.

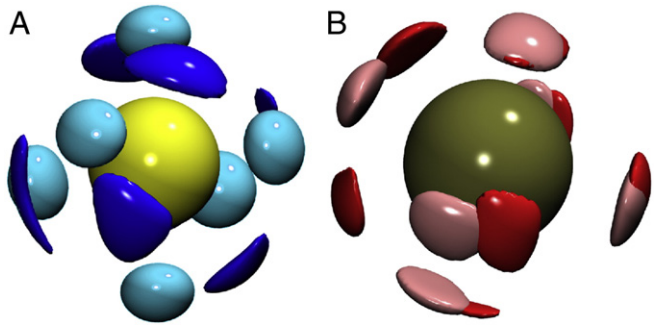

Fig. 5. (A) A comparison of the probability density maps of the oxygen positions about Na^+ with 6 (light blue) and 7 (dark blue) formaldehyde ligands. One dark blue region is obscured by the ion. (B) The same comparison for the 6 ligands (pink) and 7 ligands (red) around K^+. A large difference in the ion–ligand distance and ligand position is apparent for Na^+, but not for K^+. Before calculating each probability map, each frame is aligned to the average set of coordinates.

type, r always increases the slowest and smoothest with respect to n for K^+ meaning that the ligands show a gradual and smooth adjustment to the addition of each additional ligand. In contrast, the plots for Li^+ and Na^+ show significant jumps in the rate of increase. For example, for formaldehyde coordinating to Li^+ and Na^+ there are peaks at $n=5$ and 7, and $n=7$ respectively. In general, as the number of coordinating ligands increases, so too does the ion–ligand distance. However, Li^+ and Na^+ exhibit dramatic increases with the addition of particular ligand numbers. The sudden changes noted in the ion–ligand interaction energy are associated with these changes in the average ion–oxygen distance.

What causes the average ion–ligand distance to change with ligand number? Our results show that every time a ligand is added the size of the coordination sphere must increase to accommodate this next ligand, as is to be expected (Fig. 4). However, these results also show that this size change is not uniform, and the addition of certain ligands has a much greater effect of the size of the coordination shell than others. We believe that the reason for this is that there comes a point at which the ligands form a 'full' shell around the ion, and another ligand cannot be added without significantly adjusting the positions of all the ligands due to the ligand–ligand repulsion. Obviously this happens at a smaller ligand number for smaller ions, and so such dramatic rearrangements in the size and geometry of the coordination shell happens for Li^+ with the addition of the 5th and 7th ligands, and occur for Na^+ with the addition of the 7th ligand. Presumably a similar rearrangement would occur for K^+ at a larger ligand number. It is when these sudden changes occur that the site is likely to become selective for the larger ions.

Fig. 5 visually supports our hypothesis. Plotted are the regions in space about the ions where the oxygens dwell. With 6 formaldehyde ligands about the Na^+ ion, the oxygen atoms distribute in an octahedral geometry about the ion. However, with 7 formaldehyde ligands the positions of the oxygens change dramatically; they move further from the ion and become more localised in the radial direction. In contrast, the change from 6 to 7 formaldehyde ligands has much less influence on the oxygen positions around K^+ as seen in Fig. 5B.

To reinforce our conclusion that the ligand–ligand repulsion causes the sudden changes in geometry noted earlier, we examine what would happen if we prevent these sudden geometrical changes from occurring. To do this we impose an additional distance constraint that allows for a gradual increase in the Li^+–ligand distance with increasing ligand number, but prevents the sudden jumps as shown in Fig. 6A. In this case, once $n>6$ the total interaction energy of the system starts to become less favourable than in the unconstrained case as seen in Fig. 6B. This is a consequence of the ligand–ligand repulsion increasing more quickly than the ion–ligand attraction, highlighting that this ligand–ligand repulsion drives the geometrical change in the unconstrained system.

3. Conclusion

Ion selectivity by overcoordination is likely to arise at or above ligand numbers that require sudden rearrangements in geometry necessary to accommodate the smaller ions. This is realised through the interplay of the ion–ligand and ligand–ligand interactions as the number of coordinating ligands changes. This investigation differs from previous work [13,14,35] as it elucidates through what mechanism this interplay of interactions leads to selectivity by overcoordination, rather than simply stating that it does. This work also does not attempt to answer the questions of the role of overcoordination in particular molecules, or how molecules are able to enforce the necessary conditions for overcoordination to arise (questions 1 and 2 in the Introduction), as it is the question of how enforcing a coordination number gives rise to ion selectivity that we wish to elucidate and clarify.

Anomalous changes in coordination geometries upon the addition of extra ligands are displayed for smaller ions (Li^+ and Na^+), but not for larger ions K^+. The coordination systems reach a point where another ligand cannot be added without changing the positions of all the ligands, as there is already a 'full' shell of ligands around the ion. The discrepancy between ion types as to when these shells are 'full' results in ion selectivity by overcoordination at or above certain ligand numbers; typically upon the addition of the 5th and 7th ligands. This situation arises in each of the three types of ligands investigated in this study, although some ligand specific subtleties do arise (the propensity to hydrogen bond for example). As we have used classical molecular dynamics simulations to understand why constraining ion coordination numbers yields ion selectivity, it is possible that more detailed investigations (using

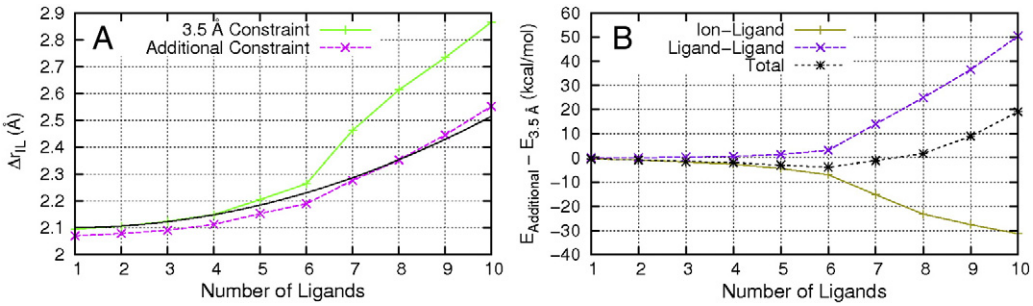

Fig. 6. (A) Average Li^+–oxygen distance for formaldehyde clusters with 3.5 Å constraint (green), with the additional constraint that prevents sudden geometrical changes (pink) and the quadratic function used to determine the additional constraint (black). (B) The differences in energy between the 3.5 Å constrained and additionally constrained clusters for the ion–ligand (dark yellow), ligand–ligand (purple) and total (black) interactions.

polarisable force fields or quantum mechanical calculations for example) may elucidate additional effects.

4. Methods

Free energy perturbation calculations were conducted within molecular dynamics simulations using model systems consisting of an ion surrounded by n water, formaldehyde or formamide molecules constrained to a 3.5 Å sphere centred on the ion using a steep-walled, flat-bottomed, one sided harmonic potential. The constraint in the additional constraint model systems that prevent the anomalous geometrical changes was determined for each n by fitting a quadratic function to $n = 1$–4. The partial charges of the formaldehyde atoms are: carbon +0.5, oxygen −0.5 and hydrogen 0.0. Water and formamide are unchanged from the CHARMM27 force field.

Ions were morphed from K^+ to Na^+ and K^+ to Li^+ over 20 λ windows of equal size run for 2 ns each (including 1 ns of equilibration), totalling 40 ns for each model system. Interaction energy and distance data were calculated by averaging the 20,000 equally-spaced samples from the first and last λ window of each simulation. The standard error involved in the distances is at most 0.07 Å. Uncertainty in ΔG, E and r of the model systems was estimated by conducting four forward and four reverse morphs ($Na^+ \rightarrow K^+$) of $n = 1$, 5 and 10 formaldehyde systems. The standard error in the mean is below 0.005 kcal/mol for ΔG, 0.12 kcal/mol for E and 0.012 Å for r. The error of $\Delta\Delta G$ is estimated to be 0.38 kcal/mol.

The exchange reaction free energies shown in Fig. 1 include relative free energies for Li^+/K^+ and Na^+/K^+ compared to bulk water. These were calculated as dehydration free energies for each ion by Joung and Cheatham [36].

Each simulation was conducted using NAMD [37] utilising the CHARMM27 [38] force field. The ion parameters are from Joung and Cheatham [36]. NAMD and in-house Fortan90 programmes were used for extracting energy and distance information. All simulations were simulated in a non-periodic toy system with no pressure or volume control, besides the 3.5 Å steep-walled, flat-bottomed, one sided harmonic potential at a temperature of 310 K with 1 fs timesteps.

Fig. 5 was created using the VolMap tool in VMD [39]. Before this, each frame was aligned to the average position of the oxygen atoms using the RMSD trajectory tool in VMD.

Acknowledgements

The authors gratefully acknowledge support of this work from the National Health and Medical Research Council (NHMRC), an award under the Merit Allocation Scheme on the NCI National Facility at the ANU and computer time from iVEC.

Appendix A. Supplementary data

Supplementary data to this article can be found online at http://dx.doi.org/10.1016/j.bpc.2012.11.005.

References

[1] B. Hille, Ionic Channels of Excitable Membranes, 3rd edition Sinauer Associates Inc., MA, 2001.
[2] G. Yellen, Ionic permeation and blockade in Ca^{2+} activated K^+ channels of bovine chromaffin cells, Journal of General Physiology 84 (1984) 157–186.
[3] L. Heginbotham, R. MacKinnon, Conduction properties of the cloned Shaker channel, Biophysical Journal 65 (1993) 2089–2096.
[4] M. LeMasurier, L. Heginbotham, C. Miller, KscA: it's an ion channel, Journal of General Physiology 118 (2001) 303–314.
[5] C.M. Nimigean, C. Miller, Na^+ block and permeation in K^+ channel of known structure, Journal of General Physiology 120 (2002) 323–325.
[6] L.J. Mullins, The penetration of some cations into muscle, Journal of General Physiology 42 (1959) 817–829.
[7] L. Mullins, An analysis of conductance changes in squid axon, Journal of General Physiology 42 (1959) 1013–1035.
[8] L. Mullins, An analysis of pore size in excitable membranes, Journal of General Physiology 43 (1960) 105–117.
[9] F. Bezanilla, C. Armstrong, Negative conductance caused by entry of sodium and cesium ions into the potassium channels of squid axons, Journal of General Physiology 60 (1972) 588–608.
[10] D. Doyle, J.M. Cabral, R. Pfuetzner, A. Kuo, J. Gulbis, S. Cohen, B. Chait, R. MacKinnon, The structure of the potassium channel: molecular basis of K^+ conduction and selectivity, Science 280 (1998) 69–77.
[11] G. Eisenman, Cation selective glass electrodes and their mode of operation, Biophysical Journal 2 (1962) 259–323.
[12] J. Åqvist, O. Alvarez, G. Eisenman, Ion-selective properties of a small ionophore in methanol studied by free energy perturbation simulations, Journal of Physical Chemistry 96 (1992) 10019–10025.
[13] S. Noskov, S. Bernèche, B. Roux, Control of ion selectivity in potassium channels by electrostatic and dynamic properties of carbonyl ligands, Nature 431 (2004) 830–834.
[14] S. Noskov, B. Roux, Ion selectivity in potassium channels, Biophysical Chemistry 124 (2006) 279–291.
[15] H. Yu, S. Noskov, B. Roux, Two mechanisms of ion selectivity in protein binding sites, Proc. Natl. Acad. Sci. U. S. A. 107 (2010) 20329–20334.
[16] B. Roux, S. Bernèche, B. Egwolf, B. Lev, S. Noskov, C. Rowley, H. Yu, Ion selectivity in channels and transporters, Journal of General Physiology 317 (2011) 415–426.
[17] M. Thomas, D. Jayatilaka, B. Corry, Mapping the importance of four factors in creating monovalent ion selectivity in biological molecules, Biophysical Journal 100 (2011) 60–69.
[18] A.N. Thompson, I. Kim, T.D. Panosian, T.M. Iverson, T.W. Allen, C.M. Nimigean, Mechanism of potassium-channel selectivity revealed by Na^+ and Li^+ binding sites within the KcsA pore, Nature Structural and Molecular Biology 16 (2009) 1317–1324.
[19] C. Nimigean, T. Allen, Origins of ion selectivity in potassium channels from the perspective of channel block, Journal of General Physiology 137 (2011) 405–413.
[20] I. Kim, T. Allen, On the selective ion binding hypothesis for potassium channels, Proc. Natl. Acad. Sci. U. S. A. 108 (2011) 17963–17968.
[21] M. Thomas, D. Jayatilaka, B. Corry, The predominant role of coordination number in potassium channel selectivity, Biophysical Journal 93 (2007) 2635–2643.
[22] D.L. Bostick, C.L. Brooks III, Selectivity in K^+ channels is due to topological control of the permeant ion's coordinated state, PNAS 104 (2007) 9260–9265.
[23] P. Fowler, K. Tai, M. Sansom, The selectivity of K^+ ion channels: testing the hypotheses, Biophysical Journal 95 (2008) 5062–5072.
[24] T. Dudev, C. Lim, Determinants of K^+ vs Na^+ selectivity in potassium channels, JACS 131 (2009) 8092–8101.
[25] H. Yu, S. Noskov, B. Roux, Hydration number, topological control, and ion selectivity, Journal of Physical Chemistry 113 (2009) 8725–8730.
[26] P.D. Dixit, D. Asthagiri, Thermodynamics of ion selectivity in the KcsA K^+ channel, Journal of General Physiology 137 (2011) 427–433.
[27] S. Varma, S. Rempe, Tuning ion coordination architectures to enable selective partitioning, Biophysical Journal 93 (2007) 1093–1099.
[28] D.L. Bostick, K. Arora, C.L. Brooks III, K^+/Na^+ selectivity in toy cation binding site models is determined by the 'host', Biophysical Journal 96 (2009) 3887–3896.
[29] D.L. Bostick, K. Arora, C.L. Brooks III, Statistical determinants of selective ionic complexation: ions in solvent, transport proteins, and other "hosts", Biophysical Journal 96 (2009) 4470–4492.
[30] D.L. Bostick, C.L. Brooks III, Selective complexation of K^+ and Na^+ in simple polarizable ion-ligating systems, JACS 132 (2010) 13185–13187.
[31] S. Varma, D. Rogers, L. Pratt, S. Rempe, Design principles for K^+ selectivity in membrane transport, Journal of General Physiology 137 (2011) 479–488.
[32] A.D. MacKerell Jr., D. Bashford, M. Bellott, R.L. Dunbrack Jr., J.D. Evanseck, M.J. Field, S. Fischer, J. Gao, H. Guo, S. Ha, D. Joseph-McCarthy, L. Kuchnir, K. Kuczera, F.T.K. Lau, C. Mattos, S. Michnick, T. Ngo, D.T. Nguyen, B. Prodhom, W.E.R. III, B. Roux, M. Schlenkrich, J.C. Smith, R. Stote, J. Straub, M. Watanabe, J. Wiorkiewicz-Kuczera, D. Yin, M. Karplus, All-atom empirical potential for molecular modeling and dynamics studies of proteins, The Journal of Physical Chemistry. B 102 (1998) 3586–3616.
[33] P.D. Dixit, S. Merchant, D. Asthagiri, Ion selectivity in the KcsA potassium channel from the perspective of the ion binding site, Biophysical Journal 96 (2009) 2138–2145.
[34] P.D. Dixit, D. Asthagiri, The role of bulk protein in local models of ion-binding to protein: comparative study of KcsA, its semisynthetic analogue with a locked-in binding site and valinomycin, Biophysical Journal 100 (2011) 1542–1549.
[35] H. Yu, C. Mazzanti, T. Whitfield, R. Koeppe II, O. Anderson, B. Roux, A combined experimental and theoretical study of ion solvation in liquid n-methylacetamide, Journal of the American Chemical Society 132 (2010) 10847–10856.
[36] I.S. Joung, T.E. Cheatham III, Determination of alkali and halide monovalent ion parameters for use in explicitly solvated biomolecular simulations, The Journal of Physical Chemistry. B 112 (2008) 9020–9041.
[37] J.C. Phillips, R. Braun, W. Wang, J. Gumbart, E. Tajkhorshid, E. Villa, C. Chipot, R.D. Skeel, L. Kale, K. Schulten, Scalable molecular dynamics with NAMD, J. Comput. Chem. 26 (2005) 1781–1802.
[38] N. Foloppe, A.D. MacKerell Jr., All-atom empirical force field for nucleic acids: 1. Parameter organisation based on small molecule and condensed phase macromolecular target data, J. Comput. Chem. 21 (2000) 86–104.
[39] W. Humphrey, A. Dalke, K. Schulten, VMD—Visual Molecular Dynamics, Journal of Molecular Graphics 14 (1996) 33–38.